



Seventh Framework Programme FP7-SPACE-2010-1
 Stimulating the development of downstream GMES services

Grant agreement for: Collaborative Project. Small- or medium scale focused research project

Project acronym: **SIDARUS**

Project title: **Sea Ice Downstream services for Arctic and Antarctic Users and Stakeholders**

Grant agreement no. 262922

Start date of project: 01.01.11

Duration: 36 months

Project coordinator: Nansen Environmental and Remote Sensing Center, Bergen, Norway

D6.4: Validation of thickness retrievals

Due date of deliverable: 31.12.2013

Actual submission date: 22.01.2014

Organization name of lead contractor for this deliverable: Norwegian Metrological Institute

| | | |
|---|--|----------|
| Project co-funded by the European Commission within the Seventh Framework Programme, Theme 6 SPACE | | |
| Dissemination Level | | |
| PU | Public | x |
| PP | Restricted to other programme participants (including the Commission) | |
| RE | Restricted to a group specified by the consortium (including the Commission) | |
| CO | Confidential, only for members of the consortium (including the Commission) | |

| ISSUE | DATE | CHANGE RECORDS | AUTHOR |
|-------|------------|----------------|---|
| 0.1 | 16.01.2014 | Version 0.1 | V. Djepa, P. Wadhams, P.Wagner, N. Hughes |

SIDARUS CONSORTIUM

| Participant no. | Participant organisation name | Short name | Country |
|-----------------|--|------------|---------|
| 1 (Coordinator) | Nansen Environmental and Remote Sensing Center | NERSC | NO |
| 2 | Alfred-Wegener-Institut für Polar-und Meeresforschung | AWI | DE |
| 3 | Collecte Localisation Satellites SA | CLS | FR |
| 4 | University of Bremen, Institute of Environmental Physics | UB | DE |
| 5 | The Chancellor, Masters and Scholars of the University of Cambridge | UCAM | UK |
| 6 | Norwegian Meteorological Institute, Norwegian Ice Service | Met.no | NO |
| 7 | Scientific foundation Nansen International Environmental and Remote Sensing Centre | NIERSC | RU |
| 8 | B.I. Stepanov Institute of Physics of the National Academy of Sciences of Belarus | IPNASB | BR |

No part of this work may be reproduced or used in any form or by any means (graphic, electronic, or mechanical including photocopying, recording, taping, or information storage and retrieval systems) without the written permission of the copyright owner(s) in accordance with the terms of the SIDARUS Consortium Agreement (EC Grant Agreement 262922).

All rights reserved.

This document may change without notice

Table of Contents

Part One

| | |
|--|-----------|
| 1 CRYOSAT-2 FOR SEA ICE THICKNESS..... | 4 |
| 2 ANALYSIS AND INTERPRETATION OF PAST UPWARD-LOOKING SONAR DATA FROM UK SUBMARINES..... | 1 |
| 2.1 INTRODUCTION | 2 |
| 2.2 ULS OBSERVATIONS | 2 |
| 2.3 RETRIEVAL OF SID FROM ULS ON SUBMARINE | 5 |
| 2.4 OPEN WATER CORRECTION OF SID | 5 |
| 2.5 BEAM WIDTH IMPACT ON RETRIEVED SID..... | 6 |
| 2.6 BIAS CORRECTED SID FROM ULS ON UK SUBMARINE | 6 |
| 2.7 CONCLUSIONS..... | 7 |
| 3 SEA ICE THICKNESS FROM SATELLITE-DERIVED DATA | 8 |
| 3.1 CRYOSAT-2 WAVEFORMS FOR SEA ICE THICKNESS DETECTION..... | 8 |
| 3.2 SYNTHETIC APERATURE RADAR (SAR) FOR SIDARUS | 9 |
| 3.3 NORWEGIAN METEOROLOGICAL SEA ICE CHARTS | 10 |
| 4 CURRENT STATUS AND FUTURE WORK..... | 13 |

Part Two

| | |
|--|-----------|
| 5 INTRODUCTION..... | 17 |
| 6 VALIDATION OF THICKNESS RETRIEVALS FROM THE IMPROVED CRYOSAT2 ALGORITHMS..... | 18 |
| 6.1 VALIDATION OF CRYOSAT 2 ALGORITHMS USING COLLOCATED SID (ULS)..... | 18 |
| 6.2 VALIDATION OF CRYOSAT-2 ALGORITHMS USING COLLOCATED SIT FROM LASER ALTIMETER..... | 20 |
| 6.3 CONCLUSIONS..... | 21 |
| REFERENCES | 22 |

SUMMARY

This document consist from two parts

Part one to evaluate the CryoSat-2 capability of distinguishing region and season specific sea ice thicknesses, and allow error bars to be determined for derived average thicknesses. Subsequently positive results from the improved algorithm would lead to implementing Cryosat-2 data into the operational processing chain to automate sea ice thickness measurements. By automating sea ice thickness products we can lessen potential errors when manually processing data. This benefits core users of the sea ice operational charts for safety in navigation, as well as the science community because they can use these archived automated products as sea ice proxies for future satellite data validations. The following summary presents the developments and results from each participant of this collaboration, as well as planned future work from the project outcome.

Part two to summarise the uncertainties and methods to derive SIT from CryoSat2, and results from validation using ULS and laser altimeter.

1) Improved CryoSat-2 algorithms have been developed. The A(FD2) algorithm decreases the uncertainty of the retrieved SIT more than 3 times and if the accuracy of the retrieved freeboard is increased the uncertainty of the A(FD2) will be decreased further. The validation of the new CryoSat 2 A(FD2) algorithm with the SID derived from ULS and the SIT from OIB laser altimeter demonstrated reduction of biases in the range from 0 to 6cm, which is not the case when the old CryoSat -2 algorithm has been used.

2) The uncertainty and sensitivity analyses show that the freeboard and sea ice density have the greatest impact on the retrieved SIT from CryoSat-2 and the impact of snow depth is the smallest one, less than the impact of snow density.

3) It was confirmed that the assumption of half snow depth over FYI will lead always to underestimation of the SIT retrieved from CryoSat 2 and is not applicable for SIT retrieval from CryoSat-2. Also it was confirmed that this assumption is based on limited OIB flights, not any validation data in 2010, using different algorithms with not proofed accuracy and use of snow depth retrieved from OIB/ radar altimeter is leading to from 1 to 3m difference in the estimated SIT from OIB laser and collocated satellite RA, which confirms that the assumption of half snow depth over FYI is wrong.

4) It was confirmed that WC is applicable over FYI and MYI and provides accurate SIT and SID retrieval from freeboard, using the A(FD2) algorithm.

Part One

1 Cryosat-2 for Sea Ice Thickness

CryoSat-2 is a radar altimetry mission that was launched in April 2010 to observe ice sheet and sea ice conditions, specifically aimed at observing trends in Arctic sea ice extent. CryoSat-2 operates in the Ku-band (13.575 GHz) and measures Earth's surface from an altitude of approximately 720 km for latitudes up to 88° for the north and south. The main altimeter is called SIRAL (SAR/Interferometric Radar Altimeter) which can operate in three different measurement modes; Low-Resolution Mode (LRM) for ice sheet interiors, SAR for sea ice floes, and Interferometric mode to observe ice sheet margins over mountain glaciers at an inclination of 92°. In CryoSat-2 pulse limited mode, a burst of radar pulses are sent at intervals of approximately 50 μ s (20000 Hz) and the echo returns are correlated for a swath of 250m wide, 15km long, and a period of 99.2 minutes. The satellite moves forward at 250m for each interval. Further specifications can be found at: <http://goo.gl/A7sSbp>

Though the use of level 2 CryoSat-2 data was preferred for this comparison due to the inclusion of multiple parameters (i.e. retracker, sea surface height, freeboard, elevation..etc.), a thorough investigation into the development schemes of level 2 data components found no clear literature as to how these were being produced and the values were found to be absent from the products. Since it is difficult to obtain an accurate mean sea surface, the isostatic balance of the ice floe in the ocean makes it difficult to measure sea ice freeboard. Freeboard is the height of the ice surface above the water line. Uncertainties from ice freeboard and density are a primary source of errors when calculating sea ice thickness (Alexandrov, V. et al 2010).

2 Analysis and interpretation of past upward-looking sonar data from UK submarines

UCAM led field campaigns to collect sea ice thickness profile measurements with the use of LiDAR to create a 3D replica of the ice surface characteristics, drill hole measurements, autonomous underwater vehicles (AUV), and submarine sonar data to collect information under ice drafts as required in WP2. Data were successfully collected from all sources except the under ice drafts due to the cancellation of the UK Navy submarine cruise, over which the project partners had no control. UCAM participated on the Greenpeace *Arctic Sunrise* cruise in 2011 and 2012 where they took LiDAR and drill hole measurements (2011) and LiDAR, drill hole, and AUV measurements (2012) of sea ice in the Fram Strait off the eastern coast of Greenland, see deliverable D.2.3 An overview of the floe thickness data (as derived from drill holes) is provided by figures one and two below for 2011 and 2012 respectively.

It should be noted that some challenges occurred due to difficulties in coordinating field experiments in terms of sampling areas or observed parameters which produced limited, but valuable, profile measurements. See D.2.3 for details (Figure 2.1 and 2.2).

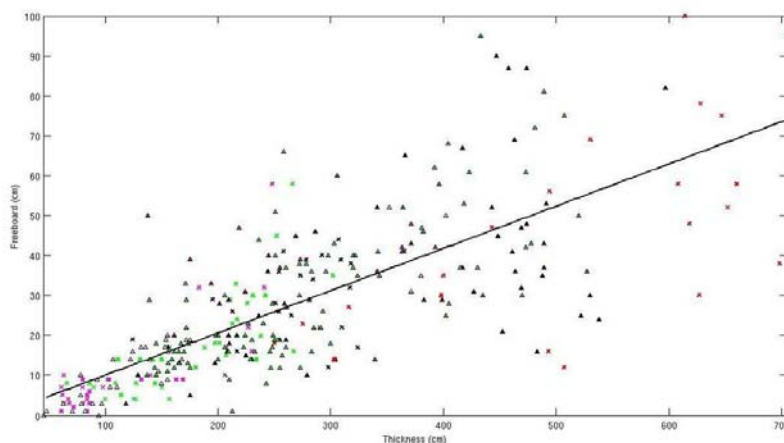


Figure 2.1. Scatter plot of floe thicknesses for AS11 campaign. Each marker represents a different floe. There are 9 floes in total, 347 data points. Y-intercept: -0.5018 cm, slope: 0.1058, correlation coefficient: 0.7535

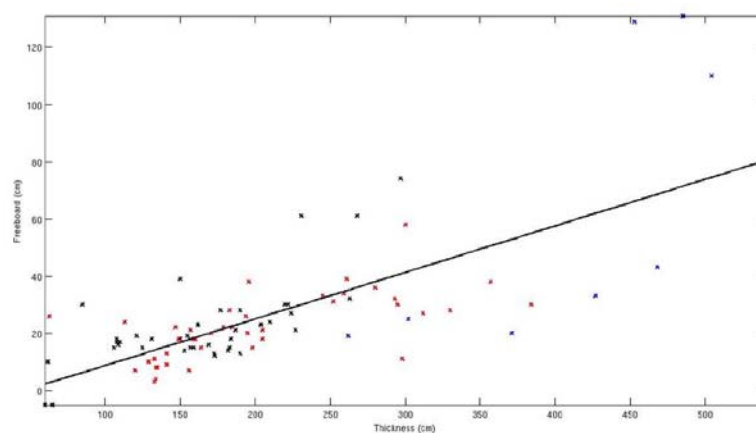


Figure 2.2. Scatter plot of floe thicknesses for AS12 campaign. Each marker represents a different floe. There are 3 floes in total, 89 data points. Y-intercept: -7.6078 cm, slope: 0.1629, correlation coefficient: 0.7267. Figure from AS12

2.1 Introduction

Sea ice thickness and draft are important climate variables for estimation of Arctic sea ice volume and validation of climate models and satellite observations (Schweiger, 2011, Rothrock et al., 2008). Data from upward looking sonar (ULS) have been used for mapping ice bottom topography and sea ice draft (SID) distribution, but still not all ULS data are processed and error corrected (Wadhams et al 2011). There are a number of environmental, random and systematic factors contributing to the accuracy of the sea ice draft derived from submarine ULS, where the open water and the impact of beamwidth are the most important errors (Rothrock and Wensnahan, 2007). Error corrections have not been applied for SID derived from ULS observations in 2007 (Wadhams et al, 2011). Considering the recent climate change and the high sensitivity of sea ice to climate variability, accurate SID data are required for initiation and validation of climate models and satellite observations. For this purpose and to provide long term, accurate data sets of climate variables, the retrieved SID in 2007 from ULS operating on a submarine in Beaufort Sea has been error corrected. The aim of this document is to analyse the existing SID derived from UK Submarines and provide a method for retrieval of SID from ULS with corresponding uncertainty analyses and error correction functions. The SID (ULS) retrieval technique, error correction algorithms and correction function for SID (ULS) derived in 2007 in the Beaufort Sea are summarised in Section 2.3 - 2.7.

2.2 ULS Observations

The *Tireless* route in April 2004 is shown on Figure 2.3/a and the submarine track in the Fram Strait on Figure 2.3/b.

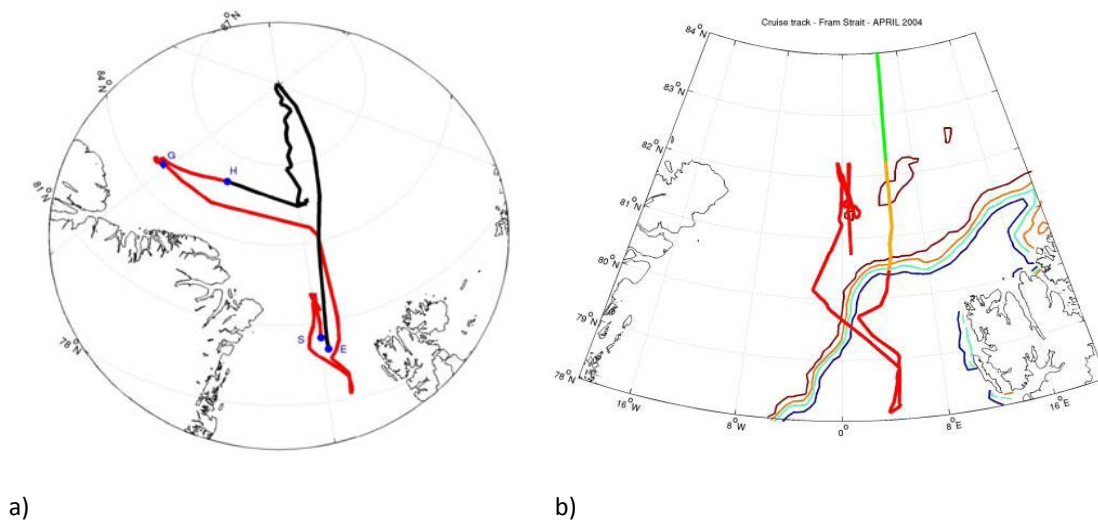


Figure 2.3. Tireless route in 2004.

The mean ice draft (with 50km spatial resolution), not corrected for open water offset and beam width impact, for 2004 is shown on Figure 2.4 and 2.5.

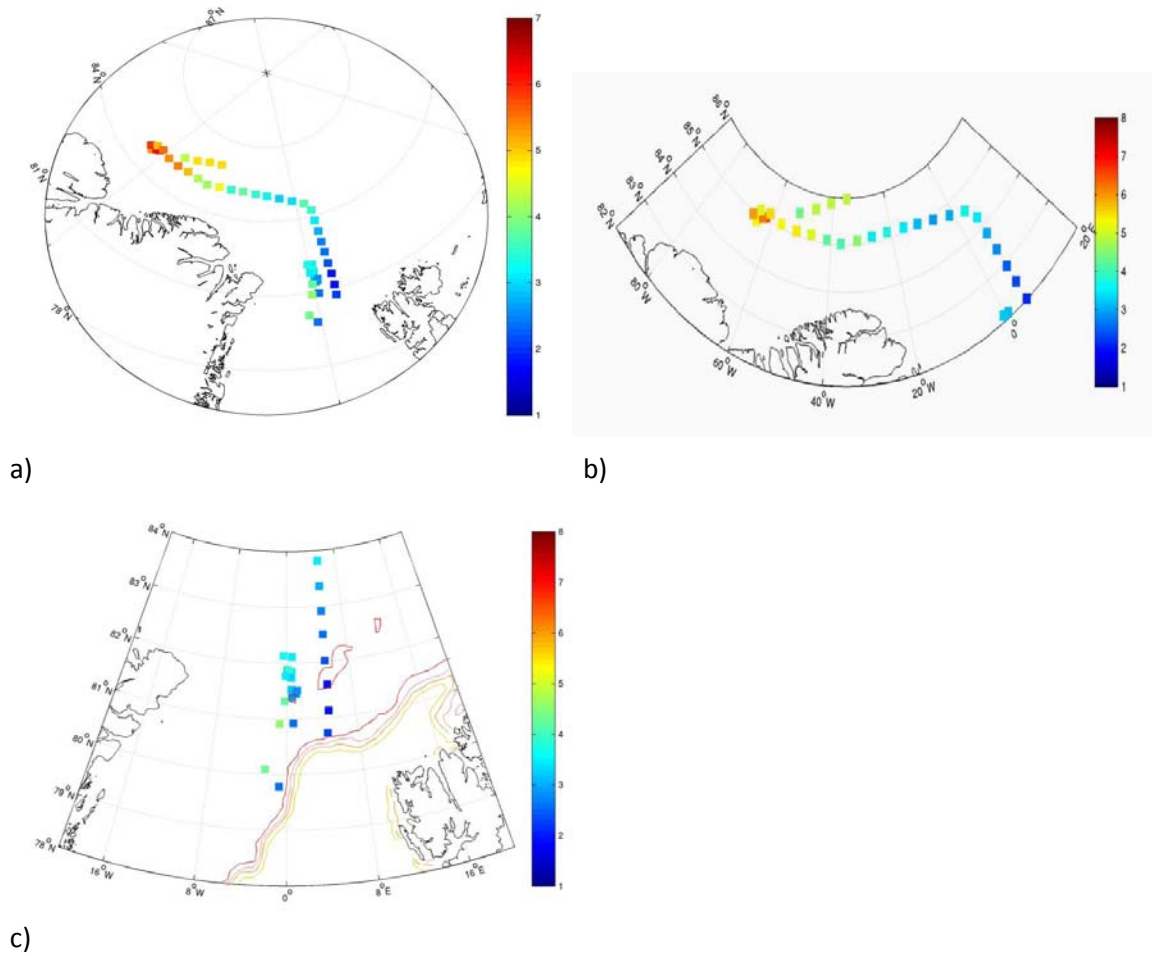


Figure 2.4. Mean Ice Draft for 2004 Cruise; b) Fram Strait; c) Greenland

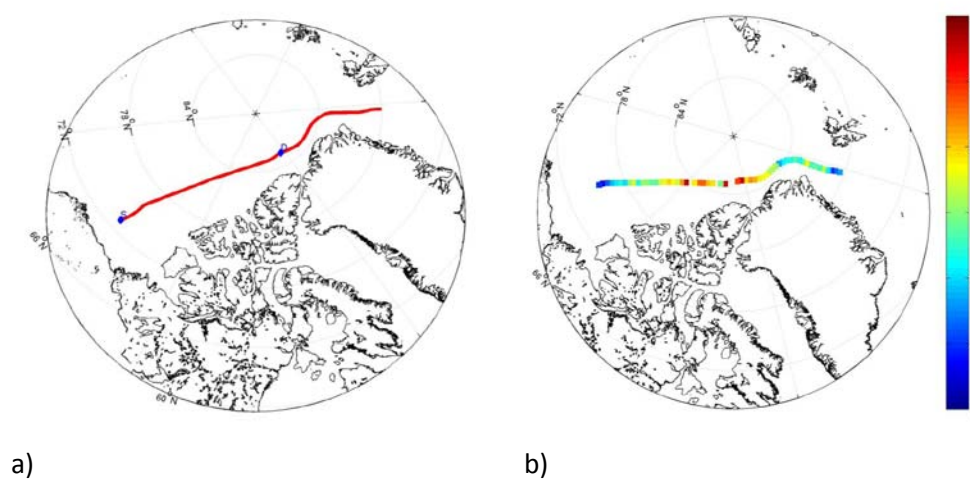


Figure 2.5. Track of the March 2007 Cruise(a) and mean SID (50km resolution) not corrected with beam width and open water offset (b).

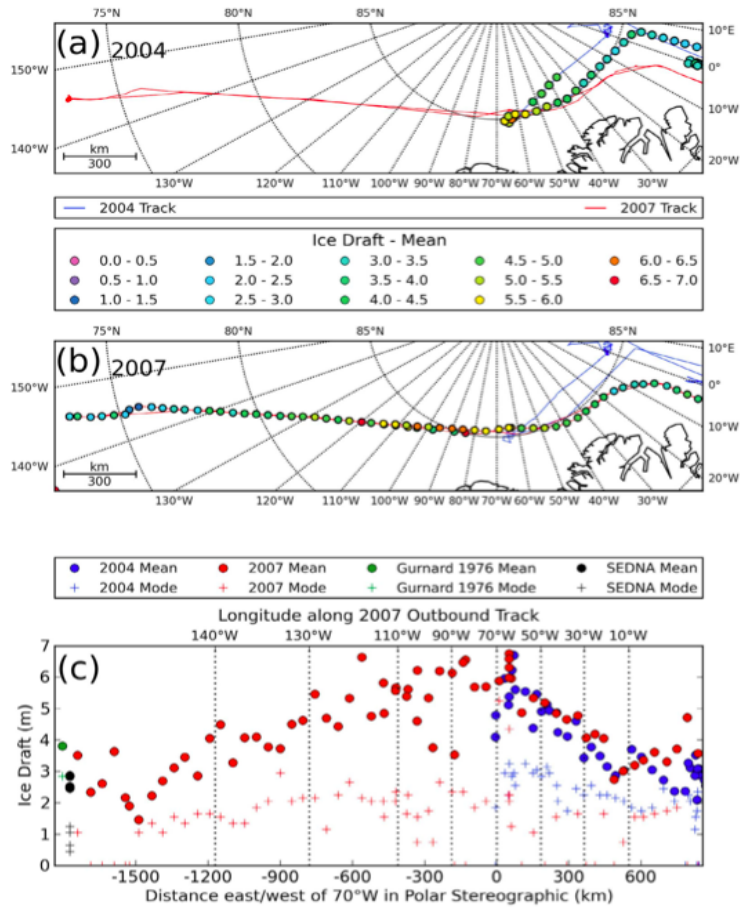


Figure 2. Color-coded mean drafts from 50 km sections of (a) 2004 and (b) 2007 cruises. (c) Mean (solid circles) and modal (crosses) drafts from 50 km sections of the 2004 cruise and 2007 outward tracks, plotted as functions of eastward distance starting from 70°W reference line in a polar stereographic projection is also shown. Black data points are from the SEDNA ice camp region, while green data point is the mean of April 1976 data from same region.

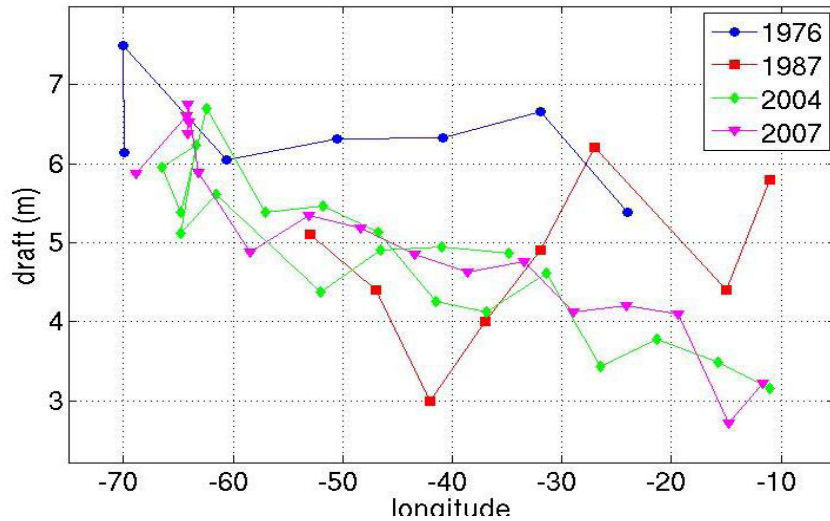


Figure 2.6. Mean ice draft for : a) 2004, 2007 Cruise; b) 4 cruises (1976, 1987, 2004 and 2007), not bias corrected.

2.3 Retrieval of SID from ULS on Submarine

The sea ice draft (d) measured by sonar transducer mounted on the submarine is calculated from the difference between the depth of the transducer (D_T) below the sea surface and the sonar measured range to the ice bottom by:

$$d = D_T - r \quad \text{equ. 2.1}$$

where $D_T = D - H$, where H is the vertical distance from the pressure sensor to the sonar transducer ($H=15.7\text{m}$ for US submarines, Rothrock and Wensnahan, 2007), and D is the keel depth, determined by the measured pressure, p and calculated as:

$$D = (p - p_a) / \rho_w g \quad \text{equ. 2.2}$$

where p_a is the local sea/atmosphere level pressure (can vary $\pm 0.3\text{ m}$), ρ_w is the water density, and g is the acceleration due to gravity.

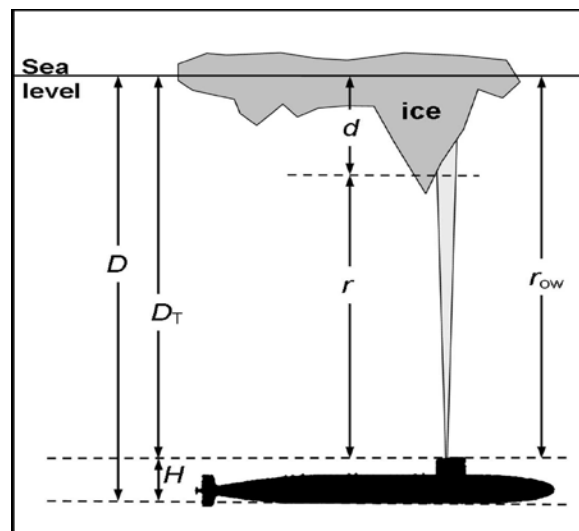


Figure 2.7. Relation of the submarine, ULS and ice draft (Rothrock and Wensnahan, 2007).

The range r is a distance to the ice, measured by $r = 2tc$, where $2t$ is the return signal as a function of time t and c is the mean sound speed in the water column. The system precision for measured draft when the boat is stationary under smooth ice, is $+6\text{ cm}$ [Rothrock and Wensnahan, 2007] and the spatial resolution is about 1 m . The error of the retrieved SID on the submarine is proportional to the speed of sound and inversely proportional to the water density. The water density varies inversely with the temperature, and the contributions of sound velocity, water density and the trim angle of the submarine are negligible, compared with the beamwidth and open water offset impact, which are the dominant factors contributing to the error of the derived SID from ULS [Rothrock and Wensnahan, 2007].

2.4 Open water correction of SID

The main sources of biases on the SID retrieved from ULS on a submarine are open water correction and footprint error. Rothrock and Wensnahan (2007) estimated mean total bias of 29 cm and standard deviation of about 25 cm for NSDIC SID (ULS) data, accounting for the footprint error of ULS (with 2σ beamwidth) and open water correction. This estimate is valid for SID retrieved from US submarines if open water correction has been applied.

Unfortunately, open water and beamwidth corrections have not been applied for SID retrieved in 2007 from ULS on the 2007 UK submarine (Wadhams et al, 2011), leading to negative bias in some regions due to wrongly identified open water in the presence of thin ice. The open water offset also

changes when the submarine changes speed or depth. The submarine depth is measured relative to sea level pressure, which changes with distance. The transducer depth impacts the accuracy of the retrieved SID along the submarine track. The presence of thin ice (up to 30 cm thickness) in the Arctic is easily mistaken for open water, leading to a negative bias. Wrongly identified open water due to the presence of thin ice, or change of the speed and depth of the submarine, could lead to bias in the retrieved SID and negative draft. Correction for open water offset of SID (ULS) derived in 2007 is required to make the SID (ULS) data comparable with SID from NSIDC, to improve the accuracy of SID (ULS) and remove the negative bias due to presence of thin ice, or unexpected change of the depth of the submarine. The algorithm for open water and beam width correction of the ULS on Submarine is given in Djepa and Wadhams, 2013.

2.5 Beam width impact on retrieved SID

Because the sonar beam is not narrow, the sonar observes an area of the under-ice surface called the “footprint”. A finite footprint diameter causes the first return to be biased toward deeper draft (d_{iFR}) compared to the mean draft within the footprint (d_{imf}) or the draft exactly in the centre of the footprint. The footprint bias varies with the nominal footprint diameter or width W_f , which in turn is proportional to the beamwidth (γ) and to the transducer depth, D_T . The impacts of geo-acoustical properties of the ice (including roughness), the range (r), transmit power, transmit and receive sensitivities are negligible. The footprint error (ε_b) depends also on ice type, roughness and slope within the footprint. Vinje et al. (1998) derived relationships between footprint error, ε_b , and the footprint width, W_f , for different ice types and roughness, which have been applied by Rothrock and Wensnahan (2007) to estimate the footprint impact on SID(ULS) for flat thin ice and beam width 2° (NSIDC ULS). A similar algorithm to that applied by Rothrock and Wensnahan (2007) for bias correction of ULS from NSIDC has been applied for bias correction of ULS on UK submarines (with beam width 3°).

2.6 Bias corrected SID from ULS on UK Submarine

The bias correction and open water offset for ULS available sections with 50km spatial resolution are shown in Figure 2.8. The raw and corrected sea ice draft, derived in March-April 2007 from ULS on a submarine in the Beaufort Sea, are compared in Figure 2.9 (Djepa, V. And Wadhams, P. 2012).

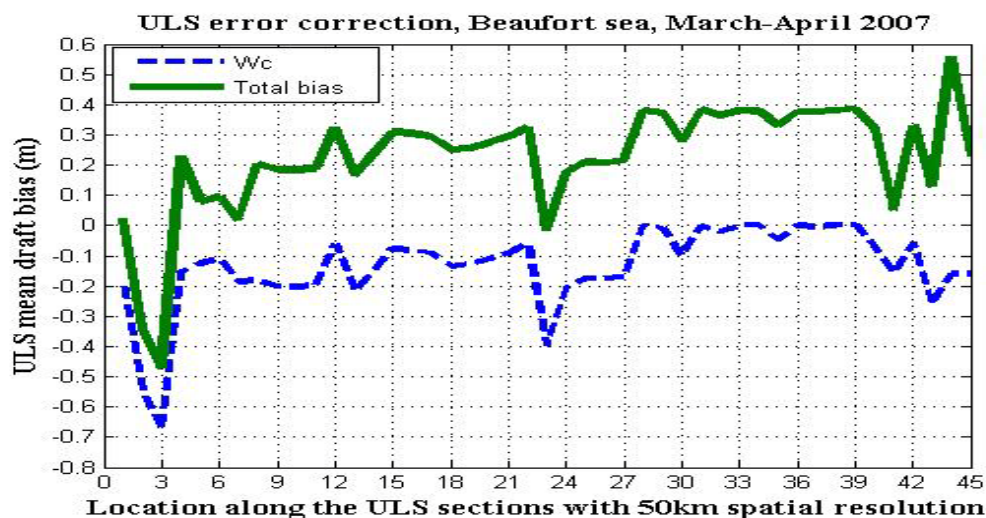


Figure 2.8. Water correction offset W_c and total bias for available data along the track of the submarine.

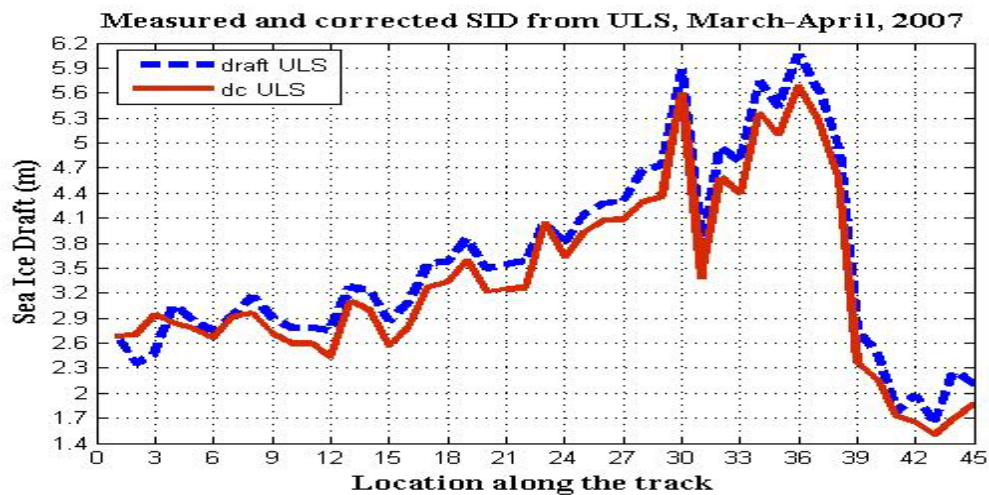


Figure 2.9. Available raw and corrected (red, solid) SID from ULS, 03/2007, along the Submarine track in Beaufort Sea.

The bias corrected SID from ULS in 2007 have been used for CryoSat-2 algorithm validation.

2.7 Conclusions

The review of available SID from UK submarines demonstrates the location of the observations. Only the available data of SID from the Beaufort Sea in 2007 are bias corrected and can be used for quantitative analyses. The rest of the data are not bias corrected and can be used only for illustration purposes.

3 Sea Ice Thickness from Satellite-derived data

Met Norway led the task of extracting relevant data from CryoSat-2 to determine how to improve its capability to detect sea ice thickness by comparing it with available in situ measurements, Synthetic Aperture Radar (SAR) data, and sea ice charts as dependent variables for ice thickness proxies. The following describes the background and application by Met Norway for each data source.

3.1 Cryosat-2 waveforms for Sea Ice Thickness detection

Average waveforms from the level 1 data were used to determine if a criteria can be established in which radar altimetry measurements can detect sea ice thickness variations based on measurements from the waveform amplitudes. Cryosat-2 SAR mode level 1b data waveforms were converted to power in Watts with knowledge of the scale factor and power. Characteristic waveforms over sea ice show rougher signatures due to the irregularity of surface features. However, indicative patterns that include new thin ice or leads should display these features as having the highest amplitudes, whereas smaller waveforms represent surface roughness. Depending on where these open water or thin ice areas occur within the waveform, this information can theoretically be used to infer sea ice thickness. Waveforms are clearly defined to determine whether the surface is ocean or sea ice (Figure 3.1). Indicative features show a small peak prior to a dramatic larger peak due to noise from the reflection of surrounding elevated features.

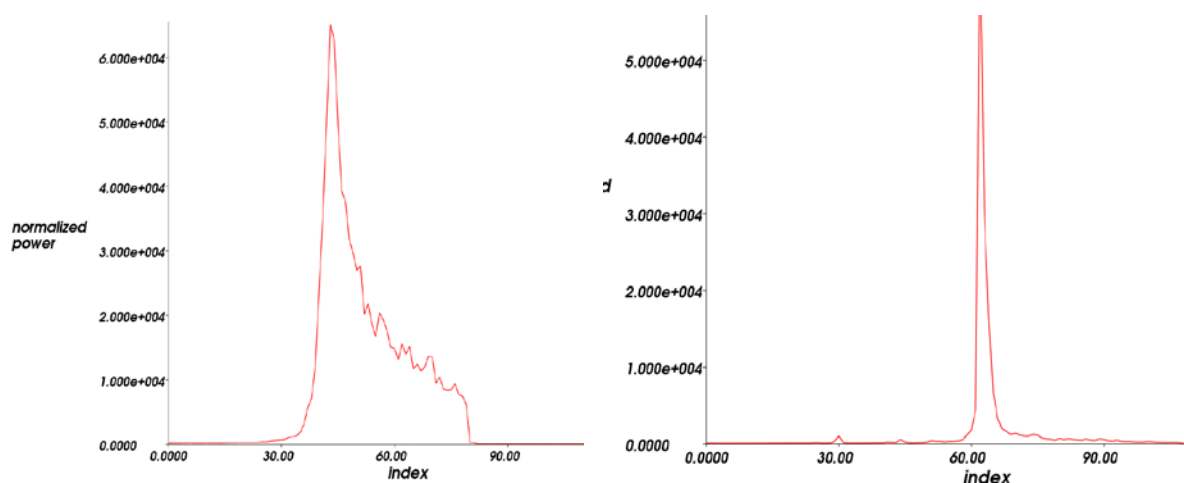


Figure 3.1. Waveforms in SAR mode over ocean (left) and over ice (right).

(http://www.altimetry.info/html/use_cases/data_use_case_cryosat_2-2_en.html)

Several passes were combined and overlain on to the Radarsat-2 SAR data to illustrate how well it can detect areas of open water (Figure 3.2).

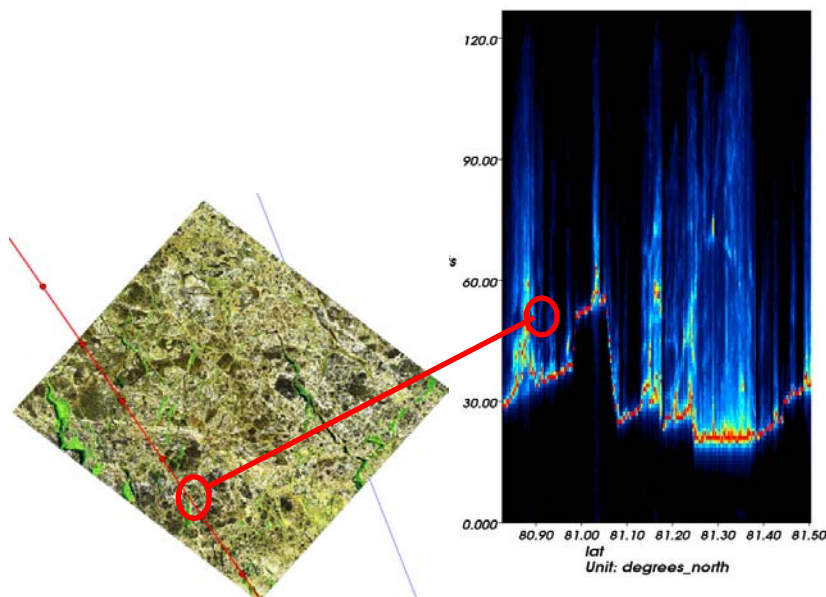


Figure 3.2. 13 April 2011 corresponding to Radarsat-2 image (left) and CryoSat-2 level 1b waveform transect (right). The red transect line shows how the waveform could be used to detect thin level ice or leads.

However, in order for these waveforms to accurately depict the surface roughness it is necessary to implement the appropriate retracking algorithm to determine at which point the waveform is actually measuring the surface from a nadir view rather than showing effects related to noise from how the signal varies in range direction. The following retracking algorithms are currently available:

1. **University College London (UCL):** ESA retracker
2. **Alfred Wegner Institute (AWI):** Threshold-Spline-Retracker Algorithm
3. **National Oceanic and Atmospheric Administrations (NOAA):** Ocean height based on Maximum Likelihood Estimator
4. **Finnish Meteorological Institute (FMI):** Open water and new ice threshold retracker with a Gaussian and Gaussian + exponential fit
5. **Traditional Offset Center of Gravity (OCOG) retracker**
6. **Primary peak OCOG retracker**

Though the above retrackers have been used with previous corrections, specific conditions require different methods of fitting the tracking point on the leading edge and the algorithms vary with each mode. The level 2 data implemented an OCOG and an OCOG threshold retracker but requires further evaluation to resolve errors in the return. Therefore, it will be necessary for Met Norway to customize our own thresholds and parameters to the level 1b data to fit our needs of doing a robust comparison with SAR and in situ data.

3.2 Synthetic Aperature Radar (SAR) for SIDARUS

Met Norway provided high-resolution SAR data to coincide with ground-truth measurements for the KV *Svalbard* cruise led by the Norwegian Polar Institute and the *Arctic Sunrise* cruises in 2011 and 2012 in which UCAM participated. The use of SAR data was included in the SIDARUS project to augment sea ice charts when delineating sea ice types and areas of deformation. Satellite data for the validation of the CryoSat-2 ice thickness product have been achieved through a national quota for RADARSAT -2 data. In addition we have had access to Radarsat-2 data from the MyOcean project

which routinely is downloaded to the national ice service at Met Norway It has therefore not been necessary to use SIDARUS data from the DWH in this validation.

The Radarsat-2 Fine Quad pol (HH+VV+HV+VH) were used for this project which covered a 25 x 25 km area with a 5-8 meter spatial resolution and an incidence angle between 18°- 49°. The Single Look Complex (SLC) beam mode data were processed using the Next ESA SAR Toolbox (<http://nest.array.ca:8080/web/nest>) to evaluate initial comparisons. Subsequently they were converted into GeoTIFF's for ease of overlaying in situ ASCII data with Cryosat-2 altimetry data in Quantum GIS.

3.3 Norwegian Meteorological Sea Ice Charts

Met Norway produces sea ice charts in the Arctic daily from several satellite-derived data to provide products pertaining to sea ice conditions that aid in navigation. These charts include information on sea ice concentration and ice edge. The ice charts are generated every day for sea ice conditions in the Norwegian Sea and the area east of Hopen. They assist in navigational purposes, as well as providing an archived dataset (<http://myocean.met.no/>). These products are derived from visible, active and passive microwave data, and actual observations when available. Met Norway has also made efforts to archive their charts. The ice charts consist of a compilation by first using charts from the previous day to keep record consistency. Subsequently, all available data is combined and placed over the previous day's ice edge sequentially with the highest resolution data first (Visible and SAR), followed by lower resolution data (passive microwave). Though SAR data is preferable, it does not always provide the global coverage needed or detect some sea ice features due to some geophysical constraints. The sea ice charts are produced by a team of analysts skilled at discerning sea ice properties with the use of Geographical Information Systems (GIS) and remotely sensed satellite data. Each analyst focuses on a specific area for continuity which allows them to have an innate familiarity with sea ice conditions in the area. New vector files are subsequently modified with current sea ice types and concentration to reflect the current day's sea ice conditions. Though sea ice analysts undergo rigorous training to observe sea ice parameters in remotely sensed data, the process is not automated which continues to introduce a certain level of uncertainty to the ice charts. The level of subjectivity with sea ice analysts is difficult to quantify; however, these charts can be used to map out the stage of development for sea ice types due to the amount of metadata included in each chart.

During the KV *Svalbard* cruise in April 2011 led by the Norwegian Polar Institute, Met Norway provided assistance with sea ice observations and support with coordinating satellite tracks with in situ measurements with the use of Radarsat-2 Quad-pol and ScanSAR Wide data for this field campaign. In conjunction with the SIDARUS project, sea ice charts were specially generated for the sea ice area north of Svalbard, Norway to coincide with the KV *Svalbard* cruise from 11-13 April. Each day, two ice analysts created sea ice charts from SAR for the same location using the same data sources in order to evaluate how the sea ice charts vary temporally and with each analyst (Figure 3.3).

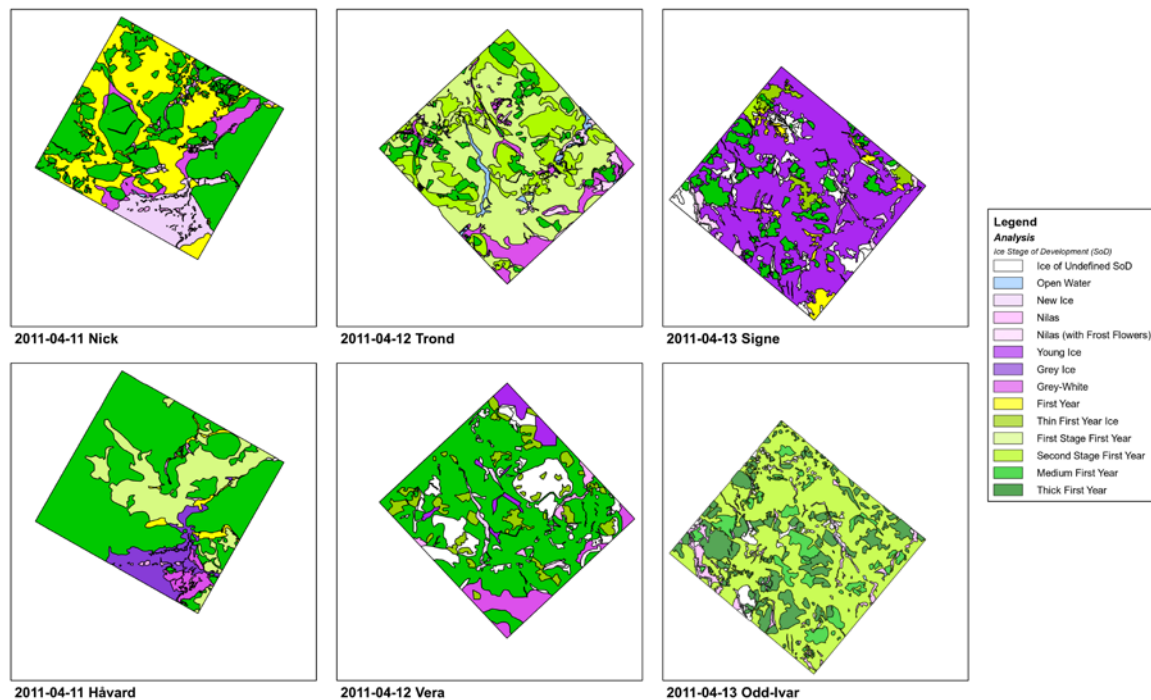


Figure 3.3. Sea ice charts for 11-13, April 2011 produced by two analysts each day to compare sea ice type interpretation.

Moen et al, 2013 quantified these differences with the ice charts from 12 April which revealed a disagreement both in segmentation (de-lineation of homogeneous regions) and classification (grouping and labelling of similar segments). Multiple levels describing first-year ice are used depending on available data at that time. However, some similarities in the segmentation correlated to several variations of first-year ice at different stages within tens of centimetres (<https://www.ec.gc.ca/glaces-ice/?lang=En&n=D5F7EA14-1&offset=2&toc=show>) which was expected. Despite the differences, this comparison shows that the sea ice charts can be used as a tool to provide a guide for sea ice type stage of development. Therefore the use of the ice charts can be used to separate first-year and second-year ice, as well as open water, but not necessarily for smaller features within the sea ice. The range of first-year ice is between 0.1 – 1.2m. For areas of deformed ice or ridges, the thickness can be greater than 2.0m. Merging first-year ice classes would provide a more homogeneous depiction of the ice conditions but they cannot be used as sole sources for sea ice thickness comparisons with Cryosat-2 because the thickness range is too coarse.

The University of Tromsø produced an automatic segmentation scheme that could potentially compliment the sea ice charts to provide a more accurate stage of development (Moen et al., 2013). Met Norway provided SAR data for 11 April 2011 that was combined with EM-31 data collected by the Norwegian Polar Institute to provide a combination of in situ data to act as a proxy for sea ice types. The optimal sea ice types chosen to be segmented are listed in Table 3.1.

Table 3.1. Sea ice types for automated segmentation scheme

| Segment Color | Stage of Development |
|-----------------|--|
| Blue/Light Blue | First- year ice |
| Brown | Different stages of development |
| Yellow | Thin ice types |
| Red | Young ice (sometimes deformed with snow cover) |

By examining sea ice through a Pauli classification, several different types of first-year ice and deformation features that are difficult to be detected by sea ice analysts can be identified (Figure 3.4).

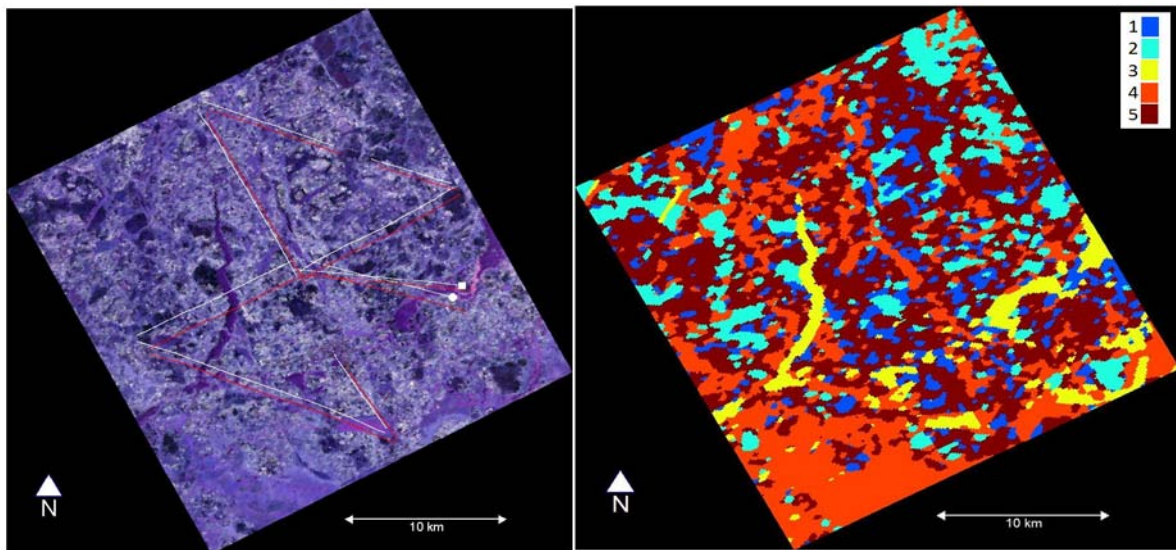


Figure 3.4. Radarsat-2 scene, 12 April 2011. (a) Geocoded polarimetry image shown as Pauli colours (the intensity channel combinations $|HH- VV|$, $2|HV|$ and $|HH + VV|$ are assigned to the RGB channels, respectively). The original helicopter track is shown in red and the drift corrected track in white. (b) Image segmented by the automated segmentation algorithm, with the number of classes set to five. (Moen et al, 2013). The first year ice types (undeformed) and sea ice under different stages of development proved to be the easiest to distinguish with this type of unsupervised classification. However, it is evident that it will take a multi-part process to separate sea ice types that tend to have similar and ridging features.

Not only can this method improve sea ice type automation, but it will make it easier to include uncertainty estimates and minimize discrepancies in first-year ice type detection shown when manually drawing sea ice charts. It would be ideal to integrate this classification algorithm within the Met.no sea ice charting system when evaluating Cryosat-2 for sea ice thickness, but it is currently in the process of being improved.

4 Current Status and future work

The first challenge of validating the Cryosat-2 radar altimetry data for sea ice thickness was substantiating data to be used as in situ measurements or ground-truth proxies. This in itself became a multi-faceted approach for the reason that in situ data is specific to sea ice conditions in the area. Though previous sea ice data records of the Arctic are available, they are not comprehensive, measured on a small scale, and do not exactly follow along the same trajectory needed for Cryosat-2 sea ice thickness validation at this time. Sea ice archives allow us to understand sea ice characteristics of a region when the data is aggregated and interpolated, but they do not allow accurate comparisons between several types of spatially and temporally differing scales.

Some challenges in evaluating dependent variables to compare with Cryosat-2 included data sources that were either still in the initial processing stages due to the natural variability of collecting sea ice data (UCAM ULS, drill hole, and LiDAR measurements); there were too much bias in the data (Met.no sea ice charts); need further processing (Radarsat-2 SAR); or were found to have parameters that were not included (Cryosat-2 level 1b and 2A data). Therefore the following description will describe future work planned as an addendum to this project.

The UCAM algorithm for open water and beam width correction of the ULS on submarine data has been completed, thus additional ULS measurements taken during the *Arctic Sunrise* cruises during 2012 can be processed using this technique. Drill hole and LiDAR measurements collected during the *Arctic Sunrise* Cruise 2011 and 2012 are in the final processing stages and will provide additional in situ data records of sea ice conditions in this area.

Cryosat-2 level 2A data currently needs further validation in order to implement the necessary sea ice thickness parameters as originally expected and stated above in section 3.1 of this document. Therefore, until these data are resolved for the level 2A data, Met Norway will continue the use of level 1b waveforms to derive freeboard estimates by evaluating the following information:

1. Retracking algorithm developed by the Finnish Meteorological Institute in January 2014.
2. Geoid changes from EGM96 to another appropriate model
3. Evaluation of UCL snow depth and density models
4. Freeboard measurements based on retracker algorithm and range measurements from waveform

The Radarsat-2 SAR data was used as a proxy for Met Norway manual sea ice charts and the UIT automatic sea ice segmentation, however, it revealed that our current level of classification is not sufficient for our purpose of determining sea ice thickness from Cryosat-2 level 1b waveforms. Met Norway will perform a robust analysis by comparing the Cryosat-2 level 1b data to the Radarsat-2 SAR data with a Maximum Likelihood supervised classification for each area where there is available in situ data (KV *Svalbard* and *Arctic Sunrise* cruises). This will allow a one-to-one comparison for Cryosat-2, as well as being able to measure the Cryosat-2 waveform along the same spatial scale (footprint). The schematic is illustrated in Figure 4.1:

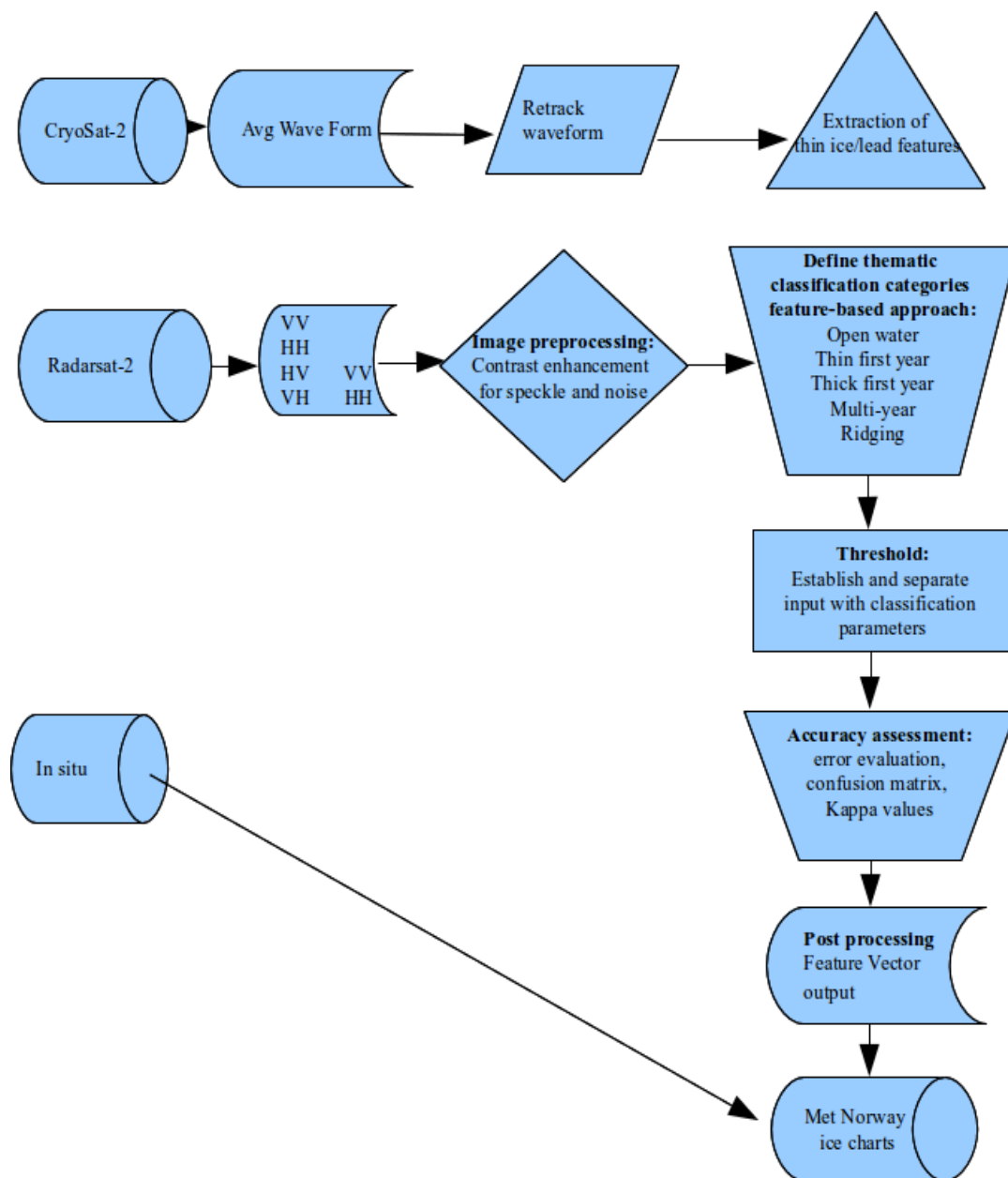


Figure 4.1. Schematic of Cryosat-2 evaluation of sea ice thickness detection for SIDARUS project.

A positive outcome of this comparison will immediately be implemented towards automation of Met Norway sea ice charts. Results will be submitted in a suitable journal for publication.

References

Alexandrov et al, (2010). The relation between sea ice thickness and freeboard in the arctic. Cryosphere Discussion.4, 641

Djepa, V. and Wadhams,P. (2012) Antarctica sea ice thickness retrieval, possible limitations, uncertainties and limitations. European Geophysical Union, General Assembly, Vienna, 07-13/14.

Moen, M. A., et al (2013). Comparison of feature based segmentation of full polarimetric SAR satellite sea ice images with manually drawn ice charts. Cryosphere, 7(6).

Rothrock, D. A., and M. Wensnahan (2007). The accuracy of sea-ice drafts measured from U.S. Navy submarines. Journal of Atmospheric and Oceanic Technology.

Rothrock,D.A., Percival,D.B., and Wensnahan, M. (2008). The decline in Arctic sea ice thickness: Separating the spatial annual, and interannual variability in a quarter century of submarine data. Journal of Geophysical Research vol. 113. C05003, doi:10.1029/ 2007JC004252

Wadhams, P., N. Hughes and J. Rodrigues. (2011) Arctic sea ice thickness characteristics in winter 2004 and 2007 from submarine sonar transects. J. Geophysical Research. 116,C00E02,doi:10.1029/2011JC006982.

Part Two

5 Introduction

The main methods for error estimation, validation and calibration of the derived SIT from satellite data are grouped in: i) experimental; ii) theoretical; iii) statistical and sensitivity analyses. Analyses of sensitivity of freeboard retrieval and freeboard-to-thickness conversion algorithm to surface variables (snow depth and density, sea ice density, sea ice type) give an estimate of the impact of input variables uncertainties on accuracy of the retrieved SIT (see D6.2, Section 2.3).

Experimental methods involve comparison of the derived freeboard and SIT retrieved from, e.g., radar altimetry with independent collocated freeboard and SIT measurements (satellite, airborne, surface, underwater) at the footprint scale. Statistical, correlation and regression analyses and comparison of the derived (gridded) sea ice product with independent SIT products from different instruments and model simulations on the same spatial and temporal scale as the SIT product have been widely applied for error estimation [R04-R06]. The same spatial and temporal resolution of the data sets is required for error analyses when collocated data sets are used. For example, within an hour, leads may open or close, deformation features may evolve, snow might be drifted away and sea ice might have drifted in different distances at the end points of a survey line, which requires precise temporal (within one hour) and spatial collocation. A time shift of one hour between satellite data acquisition, like with an altimeter, and acquisition of validation data, like in-situ drilling in combination with an over-flight of an airborne laser scanner can be enough for adding additional temporal and scale uncertainties. The spatial resolution and temporal sampling of a radar altimeter, the minimum number of altimeter measurement samples required to reduce the noise to a reasonable level, the high spatial variability of the SIT and also the minimum number of consecutive measurements to obtain a representative SIT estimate have to be considered when collocated data are used for uncertainty analyses.

6 Validation of thickness retrievals from the improved CryoSat2 algorithms

The SID and SIT retrieved from the freeboard, applying the CryoSat2 [Laxon et al, 2012] and the new developed algorithms have been validated using collocated SID(ULS) and SIT, derived from laser altimeter.

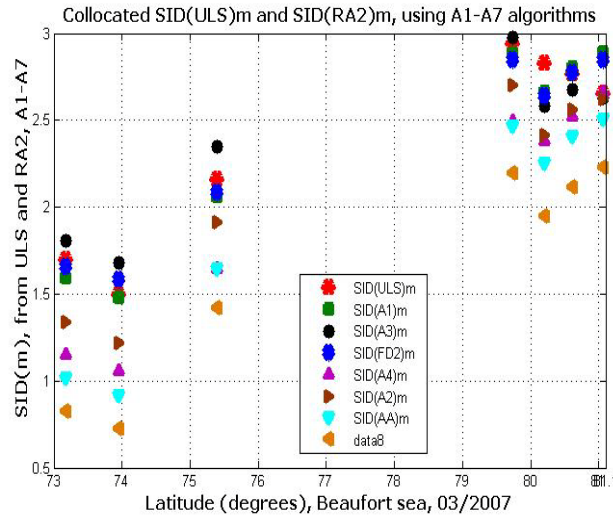
6.1 Validation of CryoSat 2 algorithms using collocated SID (ULS)

SID, calculated from the freeboard by algorithms CryoSat2 , A(FD) and A(FD2) is compared with independent SID observations from ULS in Beaufort Sea and Beaufort Gyre from 1996 to 2008 (Figure 1, Table 1).

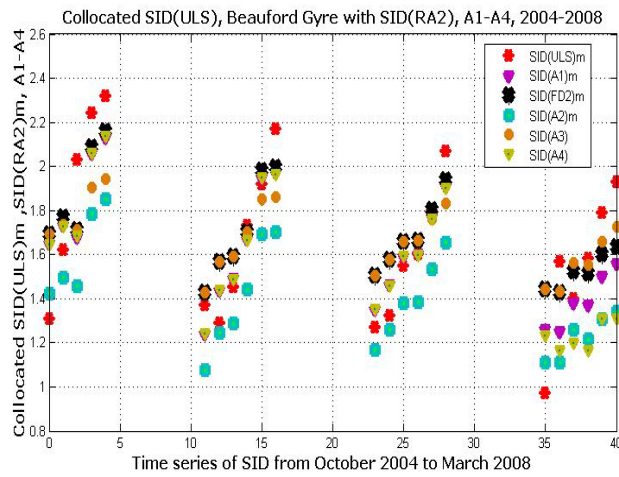
Table 1. Mean SID calculated by CryoSat 2 algorithms, collocated ULS in different locations and corresponding bias: $e = \text{SID}(\text{RA}) - \text{SID}(\text{ULS})$ in (m)

| Region | SID(A2) | SID(A(FD)) | SID(A(FD2)) | SID(ULS) | $\epsilon(\text{A2})$ | $\epsilon(\text{FD})$ | $\epsilon(\text{FD2})$ |
|--------------------------|---------|------------|-------------|----------|-----------------------|-----------------------|------------------------|
| Beaufort sea, 2007 | 2.11 | 2.386 | 2.351 | 2.365 | -0.26 | 0.02 | -0.0145 |
| Beaufort Gyre, 2004-2008 | 1.4 | 1.663 | 1.69 | 1.665 | -0.265 | -0.002 | 0.025 |
| Beaufort sea, 10/1996 | 1.567 | 1.741 | 1.74 | 1.678 | -0.111 | 0.063 | 0.062 |

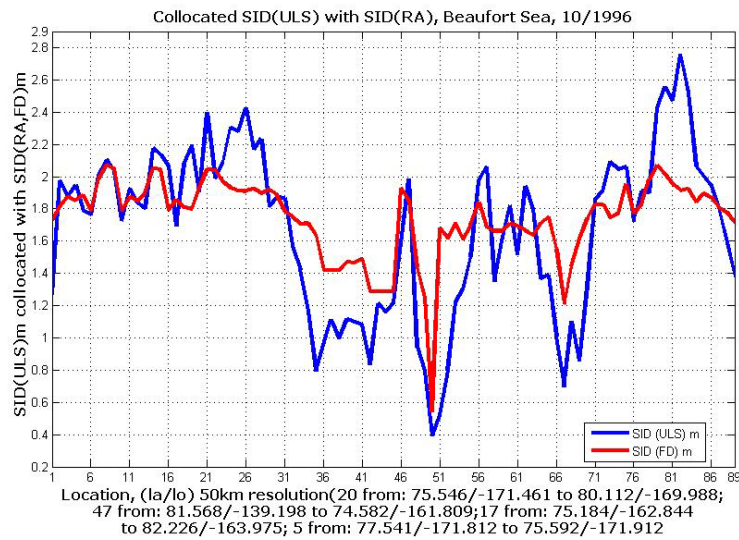
One can see that CryoSat-2 algorithm is always underestimating SID compared to SID(ULS) up to 26cm due to assumption of half snow depth over first year ice and fixed low ice density over MYI. CryoSat 2 algorithm also depends on a-priori information for presence of FYI, which is available for limited period of time since 2005 from OSI-SAF with not proofed accuracy. The developed A(FD) over MYI gives low biases but because it depends on a-priori information for presence of FYI, the A(FD2) is selected for SIT retrieval from CryoSat2 because it gives minimum biases, it does not depend on information for ice type and ice density is freeboard depended over FYI and MYI.



a)



b)



c)

Figure 1. Collocated SID (ULS) with SID(A2, CryoSat2), SID(A3, FD), SID(FD2) a) Beaufort sea 2007; b) Beauford Gyre, 2004-2008; c) Beauford Sea , 1996

6.2 Validation of CryoSat-2 algorithms using collocated SIT from Laser altimeter

The FD CryoSat-2 algorithm (A(FD2)) has been applied to retrieve SIT from laser altimeter on OIB/2010, using the equation for hydrostatic equilibrium, inserting a freeboard depended ice density and snow depth and density from WC. The statistic is summarised in Table 2. Due to use of different input variables ρ_w , ρ_s , ρ_i and h_s to calculate SIT from Laser and radar altimeter the mean bias is up to 1 m (Table 2.) and in some locations could be up to 3m, which makes impossible use of SIT derived from LA/OIB for comparison, validation or time series with SIT retrieved from RA.

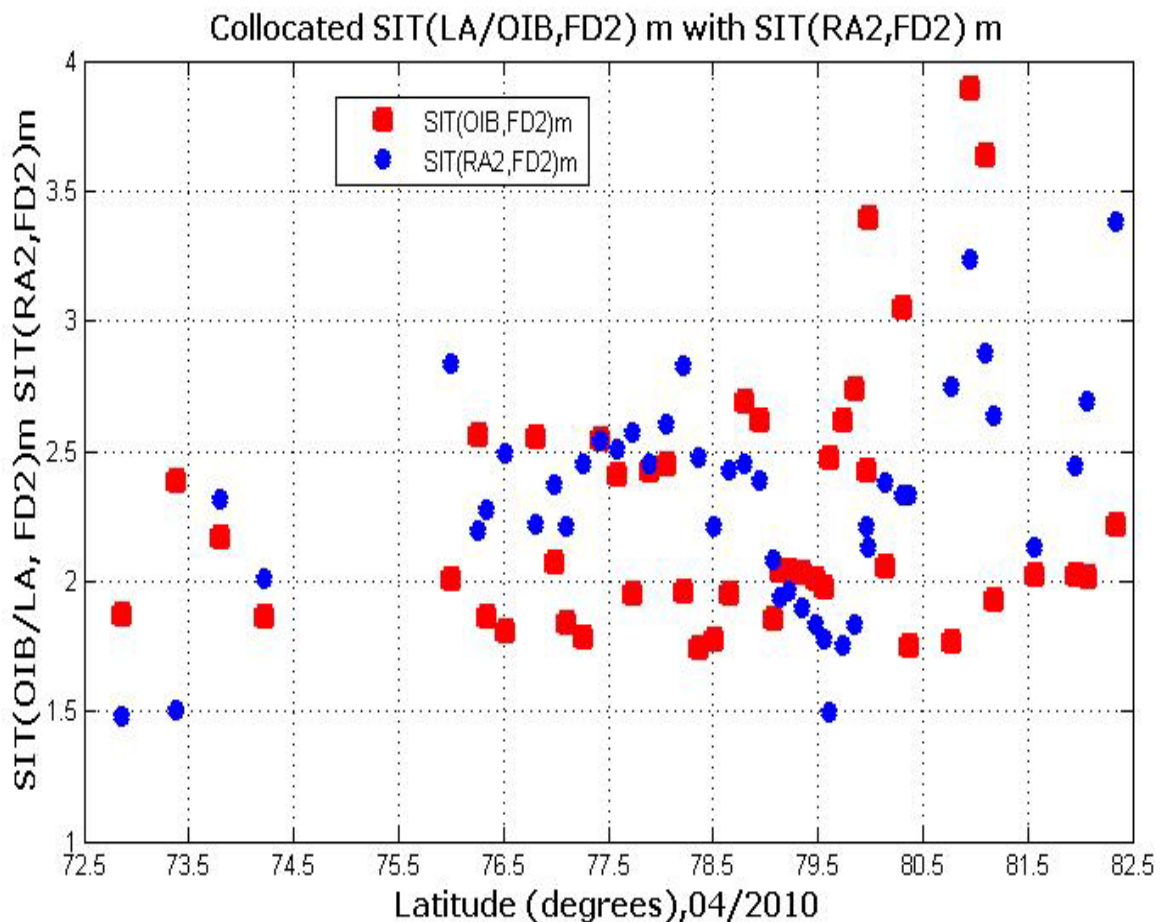


Figure 2. Collocated SIT calculated from OIB laser altimeter and RA freeboard applying the new FD2 algorithm.

The SIT derived from laser and radar altimeter applying A(FD2) algorithm is compared on Figure 2 and the statistic is given in Table 6.2. One can see that the mean bias of the SIT derived from RA2 and LA/OIB has been reduced from -1.1m for SIT calculated by RA2 and LA, using different fixed ice densities and snow depth ($e = -1.1\text{m}$) to $e = 0.05\text{m}$ when FD2 algorithm has been applied with snow depth and density from WC.

Table 2. SIT statistic for RA and LA

| Variable (m) | SIT(OIB) | SIT(RA,A1) | SIT(OIB,FD2) | SIT(RA2,FD2) |
|--------------|----------|------------|--------------|--------------|
| Mean (m) | 3.379 | 2.275 | 2.25 | 2.30 |
| Bias (m) | 0 | -1.1 | 0 | 0.05 |

The 5cm bias is within the uncertainties of the snow and ice freeboard, derived from LA and RA. The improved bias of the SIT derived by LA/OIB and RA2 when FD2 is applied confirms the improved accuracy of the FD2 algorithm for SID and SIT retrieved from LA and CryoSat-2.

6.3 Conclusions

This document summarise the uncertainties and methods to derive SIT from CryoSat2, and results from validation using ULS and laser altimeter.

1) Improved CryoSat-2 algorithms have been developed. The A(FD2) algorithm decreases the uncertainty of the retrieved SIT more than 3 times and if the accuracy of the retrieved freeboard is increased the uncertainty of the A(FD2) will be decreased further. The validation of the new CryoSat 2 A(FD2) algorithm with the SID derived from ULS and the SIT from OIB laser altimeter demonstrated reduction of biases in the range from 0 to 6cm, which is not the case when the old CryoSat -2 algorithm has been used.

2) The uncertainty and sensitivity analyses show that the freeboard and sea ice density have the greatest impact on the retrieved SIT from CryoSat-2 and the impact of snow depth is the smallest one, less than the impact of snow density.

3) It was confirmed that the assumption of half snow depth over FYI will lead always to underestimation of the SIT retrieved from CryoSat 2 and is not applicable for SIT retrieval from CryoSat-2. Also it was confirmed that this assumption is based on limited OIB flights, not any validation data in 2010, using different algorithms with not proofed accuracy and use of snow depth retrieved from OIB/ radar altimeter is leading to from 1 to 3m difference in the estimated SIT from OIB laser and collocated satellite RA , which confirms that the assumption of half snow depth over FYI is wrong.

4) It was confirmed that WC is applicable over FYI and MYI and provides accurate SIT and SID retrieval from freeboard, using the A(FD2) algorithm.

References

- R 1 Sea Ice thickness-Round Robin Data pack. User Manual Eero Rinne, M.Makynen 2012
- R2 Product Validation Plan (PVP) www.esa-cci.org, (SICCI-PVP-05-12) 1.0 2012
- R3 Sea ice thickness, freeboard, and snow depth products from Operation IceBridge airborne data. N. T. Kurtz, S. L. Farrell, M. Studinger, N. Galin, J. Harbeck, R. Lindsay, V. Onana, B. Panzer, and J. G. Sonntag Cryosphere Discussions, 6, 4771–4827. 2012
- R4 Optimization of sea ice model; using basin wide observations of Arctic sea ice thickness, extent and velocity Miller, P. A., Laxon, S. W., Feltham, D. L., and Cresswell, D. J., J. Climate, 19, 1089–1108. 2006
- R5 CryoSat: A mission to determine the fluctuations in Earth's land, marine icefield D.J.Wingham AdvS Res37, 841–871, http://www.cpom.org/research/djw-asr37.pdf 2006
- R6 Observations of ice thickness and frazil ice in the St. Lawrence Island polynya from satellite imagery, ULS, and salinity/ temperature moorings. R.Drucker, S.Martin, J. Geophysical Research,108, C5, 3149 2003
- R7 Satellite remote sensing of sea ice thickness and kinematics a review. R.Kwok, J. Glaciology, 56,200 2010
- R8 Estimation of sea ice thickness distribution through combination of snow depth and satellite laser altimeter data. http://ntrs.nasa.gov/archive/nasa/casi.ntrs.nasa.gov/20090038693_2009038644.pdf 2009
- R9 The relation between sea ice thickness and freeboard in the arctic. http://www.the-cryosphere-discuss.net/4/641/2010/tcd-4-641-2010-print.pdf; Alexandrov et al, Cryosphere Discussion.4, 641 2010
- R10 ENVISAT RA2/MWR Product Handbook http://envisat.esa.int/pub/ESA_DOC/ENVISAT/R A2-MWR/ra2 mwr.ProductHandbook.2_2.pdf 2010
- R11 AMSR-E Algorithm. Theoretical Bases Document. Sea ice product http://wwwghcc.msfc.nasa.gov/AMSR/atbd/seai2004 ceatbd.pdf, .Markus, D. Cavalieri, NASA

- R12 Snow depth on Arctic sea ice <http://seaice.apl.washington.edu/Papers/WarrenEtal99.pdf> S. Warren, I. Rigor, J. Climate, 12 1999
- R13 A review of sea ice density Timco, G. W. and Frederking, Cold Reg. Sci. Technol., 24, 1–6. 1996
- R14 Development of seasonal pack ice in the Beaufort Sea during the winter of 1991-1992: A view from below H. Melling and D. A. Riedel, J. GEOPHYSICAL RES., V. 101, N. C5, P 11, 975-11,991, MAY 15 1996
- R15 CryoSat-2 estimates of Arctic sea ice thickness and volume Laxon et al. GEOPHYSICAL RESEARCH LETTERS, V. 40, 1–6. 2012
- R16 Comparison of Envisat radar and airborne laser altimeter measurements over Arctic sea ice L. N. Connor, S. W. Laxon, A. L. Ridout, W. Krabill, D. McAdoo. Remote Sensing of Environment 113 563–570 2009
- R17 A Comparison of Snow Depth on Sea Ice Retrievals Using Airborne Altimeters and AMSR-E Simulator (http://ntrs.nasa.gov/archive/nasa/casi.ntrs.nasa.gov/20120012935_2012011929.pdf) Cavalieri, D.J., T. Markus, A. Ivanof, J.A. Miller, L. Brucker, M. Sturm, J. Maslanik, J. F. Heinrichs, A. J. Gasiewski, C. Leuschen, W. Krabill, J. Sonntag, IEEE 2012
- R18 Ice type <http://osisaf.met.no/p/ice/#type> 2012
- R19 Relationship between sea ice freeboard and draft in the Arctic Basin, and implication for ice thickness monitoring Wadhams, P., Tucker, W. B., Krabill, W. B., Swift, R. N., Comiso, J. C., Davis, R. N.: J. Geophys. Res., 97(C12), 20325–20334 1992
- R20 Airborne surveys of snow depth over Arctic sea ice Kwok, R., B. Panzer, C. Leuschen, S. Pang, T. Markus, B. Holt, S. Gogineni. J. GEOPHYSICAL RESEARCH, VOL. 116, C11018 2011
- R21 Large-scale surveys of snow depth on Arctic sea ice from Operation IceBridge Kurtz, N. T., and S. L. Farrell. Geophys. Res. Lett., 2011 38.
- R22 The decline in arctic sea-ice thickness: Separating the spatial, annual, and inter annual variability in a quarter century of submarine data D. A. Rothrock, D. B. Percival, and M. Wenshanan JOURNAL OF GEOPHYSICAL RESEARCH, VOL. 113, C05003, doi:10.1029/2007JC004252, 2008 2008
- R23 Sea ice thickness retrieval from SMOS brightness temperatures during the Arctic freeze-up period Kaleschke, L., et al., Geophys. Res. Lett., 39, L05501 2012

- R24 Estimation of the thin ice thickness and heat flux for the Chukchi Sea Alaskan coast polynya from Special Sensor Microwave/ Imager data,1990–2001 Seelye Martin and Robert Drucker, Ronald Kwok 2004 and Benjamin Holt. *J. Geophys. Res.*, 109, C10012, <http://rkwok.jpl.nasa.gov/publications/Martin.2004.pdf>
- R25 Retrieval of Thin Ice Thickness from Multi-frequency Polarimetric SAR Data Kwok, R., et al., *Rem. Sens. Environ.*, 51(3), 361- 374 1995
- R26 ICESat over Arctic sea ice: Estimation of snow depth and ice thickness Kwok, R., and G. F. Cunningham, *J. Geophys. Res.*, 113, C08010 2008
- R27 The accuracy of sea-ice drafts measured from U.S. Navy submarines Rothrock, D. A., and M. Wensnahan (2007), *Journal of Atmospheric and Oceanic Technology* 2007
- R28 Polar Remote Sensing by CryoSat-type radar altimetry Stenseng, L.: PhD 2011
- R29 Uncertainties analyses of the retrieved sea ice draft from the Upward looking sonar, operating in the Arctic V. Djepa, P. Wadhams, European Geophysical Union, General Assembly, Viena, 07-13/04 2013
- R30 Antarctica sea ice thickness retrieval, possible limitations, uncertainties and limitations Vera Djepa, P. Wadhams, ESA Symposium, November, 2012, Italy 2012
- R31 SAR and scatterometer signatures of sea ice, in *Microwave Remote Sensing of Sea Ice*, edited by F. D. Carsey, AGU Geophysical Monograph 68, 1st ed., chap. 5, Washington DC. 1992
- R32 The physical basis for sea ice remote sensing, in *Microwave Remote Sensing of Sea Ice*, edited by F. D. Carsey, AGU Geophysical Monograph 68, 1st ed., chap. 3, Washington DC. 1992
- R33 Ablation patterns of snow cover over smooth first-year sea ice in the Canadian Arctic J. Iacozza, D. G. Barber 2001
Hydrological Processes
15, 3559–3569 (2001) DOI:10.1002/hyp.1037
- R34 Arctic sea ice thickness characteristics in winter 2004 and 2007 from submarine sonar transects. Wadhams, P., N. Hughes and J. Rodrigues. 2011
J. Geophysical Research, 116, C00E02, doi:10.1029/2011JC006982
- R35 Laboratory measurements of radar backscatter from bare and snow Beaven, S. G., G. L. Lockhart, S. P. Gogineni, K. Jezek, A. R. Hosseinmostafa, A. J. Gow, D. K. 1995

- covered saline ice sheets. Perovich, A. K. Fung, S. Tjuatja.
- R36 Rapid reduction of arctic perennial sea ice. doi:10.1029/2007GL031138. Nghiem, S. V., I. G. Rigor, D. K. Perovich, P. Clemente-Colón, and J. W. Weatherly. *Geophys. Res. Lett.*, 34, L19504, 2007
- R37 Thickness and roughness variations of Arctic multiyear sea ice, Ackley, S. F., W. D. Hibler III, F. Kuzruk, A. Kovacs, and W. F. Weeks, 1976
- R38 A model for thermodynamic growth of sea ice in Numerical investigations of climate Semtner A.J. *Journal of Physical Oceanography*, v6, May 1976
- R39 Large decadal decline of the Arctic multiyear ice cover Comiso, J. C.. *J. Climate*, 25, 1176-1193 2012
- R40 Review of the microwave dielectric and extinction properties of sea ice and snow. Hallikainen, M., *Geoscience and Remote Sensing 1992 Symposium, IGARSS 92, International*, v. 2, p. 961-965.
- R41 Laboratory measurements of radar backscatter from bare and snow covered saline ice sheets Beaven, S., G. Lockhart, S. Gogineni, A. Hosseinmostafa, K. Jezek, A. Gow, D. Perovich, A. Fung, S. Tjuatja, *Int. J. Rem. Sens.*, 16(5), 851-876 1995
- R42 Monitoring ice thickness in Fram Strait. Vinje, T., N. Nordlund, and A. Kvambekk, J. *Geophys. Res.*, 103, 10 437-10 450. 1998
- R43 Arctic-Scale Assessment of Satellite Passive Microwave Derived Snow Depth on Sea Ice using Operation IceBridge Airborne Data *Journal of Geophysical Research: Oceans*, DOI 10.1002/jgrc.20228, L. Brucker, T. Marcus 2013
- Comparison of sea-ice freeboard distribution from aircraft data and CryoSat-2. Ricker, R., S. Hendricks, V. Helm, R. Gerdes and H. Skourup: *Proceedings paper, 20 years of progress in radar altimetry, 24-29 Sep., Venice, Italy*, 2012. 2012
- R44
- R45 Arctic-Scale Assessment of Satellite Passive Microwave Derived Snow Depth on Sea Ice using Operational IceBridge Airborne Data Ludovic Brucker, Thorsten Markus, *Journal of Geophysical Research: Oceans* DOI10.1002/jgrc.20228, 2013 2013
- R46 A First Assessment of IceBridge Snow and Ice Thickness Data over Arctic Sea Leuschen, T. Markus, D.C. McAdoo, B. Panzer, J. Farrell, S.L., N.T. Kurtz, L. Connor, B. Elder, C. 2012

| | | | |
|-----|--|--|------|
| | Ice | Richter-Menge, J. Sonntag | |
| R47 | Ice Physics | Hobbs, P. V., Oxford University Press, 837 pp., New York, | 1974 |
| R48 | A review of sea ice density. | Timco, G. W. and Frederking. Cold Reg. Sci. Technol., 24,1–6 | 1996 |
| R49 | Engineering properties of sea ice | Schwarz, J., and W. F. Weeks, . Glaciol., 19(81), 499-530 | 1977 |
| R50 | The ice transport through the Fram Strait, | Vinje, T. E., and O. Finnekasa, , Skr. Norsk Polarinst., 186, 1986. | 1986 |
| R51 | Development of an airborne sea ice thickness measurement system and field test results, CRREL | Kovacs, A., and S. J. Holladay. Rep. 89-19, U.S. Army Cold Regions Res. and Eng. Lab., Hanover, N. H. | 1989 |
| R52 | On the mass and heat budget of Arctic sea ice, Arch | Untersteiner, N., Meteorol. Geophys. Bioklimatol. Ser. A, Meteorology Geophysics, 2(2), 151-182 | 1961 |
| R53 | Observation on the physical properties of sea ice at Hopedale, Labrador | Weeks, W. F., and O. S. Lee, 1958. , Arctic, (3), 134-155 | 1958 |
| R54 | Combined airborne laser and radar altimeter measurements over the Fram Strait in May 2002. | Giles, K. A., S. W. Laxon, D. J. Wingham, D. W. Wallis, W. B. Krabill, C. J. Leuschen, D. McAdoo, S. Manizade, R. K. Raney. Remote Sens. Environ., 111, 182–194 | 2007 |
| R55 | Ku-band radar penetration into snow cover on arctic sea ice using airborne data | Willatt, R., S. Laxon, K. Giles, R. Cullen, C. Haas, and V. Helm, Ann.Glaciol.,52(57), 197-205 | 2011 |
| R56 | Effects of surface roughness on sea ice freeboard retrieval with an airborne ku-band SAR radar altimeter | Hendricks, S., L. Stenseng, V. Helm, and C. Haas, . In 30th IEEE International Geoscience and Remote Sensing Symposium, IGARSS, July 25-30, 2010. | 2010 |
| R57 | A thermodynamic model for estimating sea and lake ice thickness with optical satellite data | Wang X., Jeffrey R. Key, and Y. Liu. J. Geophysical Research. v. 115, C12035, doi:10.1029/ 2009JC005857, p.1-14. | 2010 |

| | | | |
|-----|--|--|------|
| R58 | BGOS ULS Data Processing Procedure | Krishfield R., A. Proshutinky. Report | 2006 |
| R59 | Passive microwave algorithms for sea ice concentration - A comparison of two techniques | Comiso, J. C., D. J. Cavalieri, C. L. Parkinson, and P. Gloersen, Remote Sens. Env., 60, 357-384. | 1997 |
| R60 | Arctic sea ice freeboard from IceBridge acquisitions in 2009: Estimates and comparisons with ICESat. | Kwok, R., G. Cunningham, S. S. Manizade, W. Krabil Journal of Geophys. Research 117:C02018. doi:10.1029/2011JC007654 | 2012 |
| R61 | The relation between Arctic sea ice surface elevation and draft: a case study using coincident AUV sonar and airborne scanning Laser | Doble, M. J., Skourup, H., Wadhams, P., Geiger, C. J. Geophys. Res., 116, C00E03,10.1029/2011JC007076, 2011 | 2011 |
| R62 | Combined airborne laser and radar altimeter measurements over the Fram Strait in May 2002 | Giles, K., Laxon, S., Wingham, D., Wallis, D., Krabill, W., Leuschen, C., McAdoo, D., Manizade, S., Raney, R.: Remote Sens. Environ., 111, 182-194, | 2007 |
| R63 | ASIRAS airborne radar resolves internal annual layers in the dry-snow zone of Greenland | R. L. Hawley, E. M. Morris, R. Cullen, U. Nixdorf, A. P. Shepherd, D. Wingham, Geophys. Research Letters, V. 33, L04502, doi: (http://epic.awi.de/Publications/Haw2006a.pdf), 10.10292005GL025147 | 2006 |
| R64 | CryoVEx 2011 Campaign Implementation Plan | Kjetil Lygre, M. Davidson, Duncan Wingham. Report | 2010 |
| R65 | Evaluation of AMSR-E snow depth product over East Antarctic sea ice using in situ measurements and aerial photography (doi: 10.1029/ | Worby, A. P. , Thorsten Markus, A. D. Steer, V. I. Lytle, R. A. Massom, J. Geophysical Res., 113, C05S94, 2007JC004181 | 2008 |
| R67 | ECMWF's Global Snow Analysis: Assessment and Revision Based on Satellite Observations | Matthias Drusch, D. Vasiljevic, P. Viterbo. American Meteorological Society, AMS, v43, 9/09 | 2004 |
| R68 | The Changing Face of Arctic Snow Cover: A Synthesis of Observed and Projected Changes | Callaghan, T. V. , M. Johansson, Daqing Yang, Ambio, 40, 17-31 | 2011 |
| R69 | Hydrographic changes in the Canada Basin of the Arctic Ocean, 1979-1996 | H. Melling, Journal of Geophysical Research, V. 103, C4, P.7637-7645, 15/4. | 1998 |

- | | | | |
|-----|---|--|------|
| R70 | Sea ice draft in the Weddell Sea, measured by upward looking sonars. | A. Behrendt, W. Dierking, E. Fahrbach, and H. Witte, Earth Syst. Sci. Data Discuss., 5, 805-51 | 2012 |
| R71 | Ice in the Ocean. Amsterdam, | P. Wadhams, The Netherlands: Gordon and Breach, 368pp | 2000 |
| R72 | Thinning and volume loss of the Arctic Ocean sea ice cover: 2003–2008 | R. Kwok, G. F. Cunningham, M. Wensnahan, I. Rigor. H. Zwally, D. Yi, J. Geophys. Res., 114, C07005, doi:10.1029/2009JC005312 | 2009 |
| R73 | The snow cover of the Arctic basin | Radionov, V., Bryazgin N., Alexandrov E., Report 1997 | 1997 |
| R74 | Sea ice thickness retrieval algorithms based on in situ surface elevation and thickness values for application to altimetry | Cicek B. O., Stephen Ackley, Hongjie Xie, Donghui Yi, and Jay Zwally. J. Geophysical Research, Oceans, v118, 3807-3822. | 2013 |
| | AWI CryoSat-2 Sea ice thickness Data product. | Hendricks S., R. Ricker, V. Helm Alfred Wegener Institute for Polar and Marine Research | 2013 |
| R75 | | | |
| R76 | Uncertainty analysis of the retrieved sea ice draft from upward looking sonar and its application for validation of the sea ice thickness derived from laser and radar altimeters | V. Djepa, P. Wadhams, under review | 2013 |

END OF DOCUMENT